1st IMEKO TC-4 International Workshop on
Metrology for Geotechnics
Benevento, Italy, March 17-18, 2016

# Small strain stiffness evolution of reconstituted medium density chalk

G. Bialowas[1], A. Diambra[2], D.Nash[3]

*Bristol University department of Civil Engineering, University Walk, Bristol BS8 1TR, UK*
*[1] e-mail) g.bialowas@bristol.ac.uk*
*[2] e-mail andrea.diambra@bristol.ac.uk*
*[3] e-mail david.nash@bristol.ac.uk*

***Abstract* – The mechanical behaviour of reconstituted chalk deposited has been investigated in a comprehensive experimental campaign using measurement and dynamic testing in the form of bender elements. Characterisation of the small strain shear stiffness ($G_0$) of this material has been performed over a range of the isotropic stress levels and over-consolidation ratios. A variation of ($G_0$) with current stress and overconsolidation ratio is, for the first time, proposed for this material. Following the widespread idea that the process of remoulding chalk may release calcium carbonate, which provides a cementing agent for grain contact overgrowth, the $G_0$ evolution at the constant stress state, over time, has been investigated for curing periods up to 23 days. Regardless of the previous stress path history prior to curing, an increase of the small strain shear stiffness with time was observed under a constant effective stress condition. This appeared to be partly associated with creep (or secondary) deformation but further increase was also observed when measurable creep deformations ceased.**

## I. INTRODUCTION

Intensive compaction and/or shearing of cemented sedimentary rock typically results in crumbling of the chalk's intergranular structure and formation of silt- and clay-sized granular material [1]. Introduction of small quantities of the reconstituted granular material within chalk significantly deteriorate the strength and the stiffness of the block [2]. This is best represented by the pile tests on chalk presented in [3], where lower shaft resistance was reported for the driven piles when compared to the board type installations. These reports have demonstrated the relevance of understanding the properties' of remoulded chalk.

Clayton [4] demonstrated using triaxial apparatus that the cohesion of the remoulded chalk might increase with time if the sample is left under constant stress conditions. Lord [3] observed the increases to shaft resistance strength of the continuous flight auger (CFA) piles over time. These all suggest the potential of chalk strength and/or stiffness self-regeneration within the engineering stress range if specific environmental conditions are attained.

Among the literature there is a strong belief that the post-deposition process responsible for the chalk formation are similar to processes governing the post-remoulding recementation. Numerous publications have thoroughly discussed the importance of the diagenetic processes undergone during ooze to chalks transformations [5, 6, 7 and 8]. All the authors consider the diagenesis to proceed in a number of successive steps (mechanical compaction, contact cement formation and cementation in form of recrystallization) following the change of ambient conditions the material is exposed to.

Fabricus [7] has demonstrated the suitability of non-destructive dynamic soil testing methods, to determine the changes to the soil stiffness at different diagenetic stages. The P-wave propagation data, obtained at various sites, has enabled the author to conclude that the progressive recrystallization of the chalk results in a stiffness increase due to difference in texture.

This paper will present the results of an experimental campaign which aimed to determine the relationship between chalk stiffness and confining stress level and investigate change of stiffness due to both secondary consolidation and potential recrystallization in reconstituted chalk samples kept under constant isotropic stress. Piezo-ceramic transducer in form of bender elements were used to assess the wave propagation velocity and the initial small strain stiffness of laboratory crashed chalk.

## II. BACKGROUND

Several laboratory techniques have been developed to measure the small strain properties of soils and the majority of these techniques rely on using wave propagation velocity to evaluate the elastic properties of the soil column [9, 10, 11, and 12].

ISBN: 978-92-990075-0-1

Bender Elements (BE) tests are the most commonly used method for laboratory testing because of the apparent simplicity of the test, the low cost of installation and the relative ease of incorporating the system within existing equipment [12]. It is well established that the initial shear modules ($G_0$) of soils under isotropic stress conditions, depends on the stress state and loading history:

$$\frac{G_0}{p_a} = S \cdot f(e) \cdot OCR^k \cdot \left( \frac{p'}{p_a} \right)^n \qquad (1)$$

where a function of the void ratio ($f(e)$), the mean effective stress ($p$') and the over-consolidation ratio ($OCR$), all account for the overall stress history of the soil [10, 13 and 14]. The atmospheric pressure ($p_a$) is introduced for dimensional consistency. The remaining symbols ($S$, $k$ and $n$) are the dimensionless material parameters, governing $G_0$ value of the soil, which account for the soil fabric and structure. It is well established that for a sample under isotropic stress condition, the current value of $p$' and the $OCR$ are sufficient enough to describe the state of the soil. Therefore, Viggiani and Atkinson [14] proposed a modification to the expression for $G_0$:

$$\frac{G_0}{p_a} = S^* \cdot \left( \frac{p'}{p_a} \right)^{n^*} \cdot R^m \qquad (2)$$

where the dimensionless material parameters are as before, but magnitude and over-consolidation ratio ($R$) is now defined as $p_y/p'$. The mean effective stress ($p_y$) is determined at the intercept between the over-consolidation line and the virgin isotropic compression line for the sample.

## III. MATERIAL, SAMPLE PREPARATION AND APPARATUS.

### *A. Reconstituted Chalk*

Margate chalk collected from the outcrop quarry in Birchington Kent was investigated. The chalk was oven dried for 24 hours at a constant temperature of 105°C prior to crushing. Subsequently, chalk rocks were crushed using a plastic mallet and then further fragmented using a hand disc grinder. Finally, the resulting gravel was passed through a Jaw Crusher BB 100 at the specific Jaws arrangements for further crushing.

The Particle Size Distribution (*PSD*) for the material (Fig.1) was obtained using a *Mastersizer* (MS) 3000 in accordance with the current standards and recommendations published by Hartwig and Loeppert [15] and Storti and Balsamo [16].

The particle sizes measured for the crushed chalk were classified as the well-graded silty clay with occasional sand size grains. The measured coefficient of uniformity (*Cu*) and the coefficient of curvature (*Cc*) were equal to 12.5 and 1.13 respectively. The obtained *PSD* curve for the crushed chalk fairly accurately corresponds with the assumed *PSD* curve for the bioclasts during chalk formation (Fig.1) as analysed by Clayton [1].

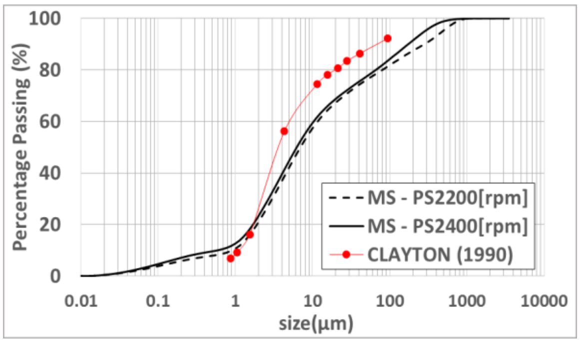


*Fig. 1. PSD curves for the crushed chalk obtained from testing and literature [1].*

*Table. 1. Atterberg values for Margate chalk.*

| Property | Measured value (%) |
|---|---|
| Liquid limit (*LL*) | 31.0 |
| Plastic Limit (*LP*) | 24.4 |
| Plastic Index (*PI*) | 6.6 |

The obtained Attenberg limits for the chalk classified the soil as CL-ML (Table.1). This information confirmed the origin and the period of the deposition of the investigated material. Margate chalk is classified in literature as a grade B2/B3 medium density; upper deposition chalk with typical index properties of the Senonian formation. The material is almost completely composed of calcium carbonates, with less than 2% impurities. The specific gravity of the material (*Gs*) is 2.70 [2].

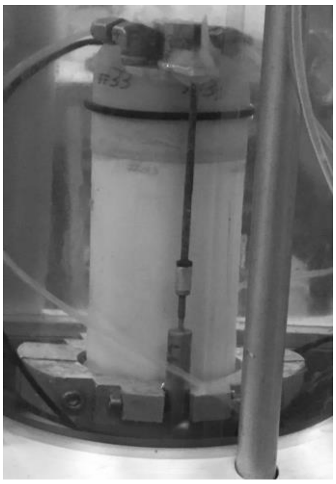

*Fig. 2. Chalk sample in triaxial setup.*

*B. Reconstituted sample preparation and saturation*

Triaxial tests were performed on 100 mm high and 50mm diameter cylindrical samples, prepared using the one-dimensional (1D) preconsolidation of slurry in an external consolidometer [17, 18].

To obtain the pouring slurry, the dried material was sieved into a bowl and mixed thoroughly to 2.2 times the *LL* (Table.1) with de-ionised, degassed water which was previously infused with chalk in order to avoid any chalk material dissolution during testing. The slurry was then carefully poured into a bottom closed funnel and placed into a degassing chamber for 180 minutes to remove any entrapped air bubbles. Small rhythmical vibrations were applied to facilitate bubble removal. The infusion of the mixing water was done by adding small amounts of the crushed chalk to the de-ionised water, and then leaving the solution in the dark for at least 14 days, before usage. After degassing, the sample was poured into a 50mm internal diameter consolidometer tube and an initial 20kPa of normal stress was applied. This normal pressure was then incrementally increased in successive stages, upon completion of consolidation. Floating cylinder consolidometers were used to minimise the effects of the shaft friction [18]. Finally, the wet chalk sample was extruded from the consolidation tube and moved onto the pedestal of the triaxial cell, where a rubber membrane is slid over it and the sensors were attached.

Before sample testing commences, the porous discs and back pressure (*BP*) pipes awere flashed with the infused, deaerated water, to remove entrapped air bubbles from the system. The *BP* applied to the samples was then gradually increased, keeping the constant mean effective stress (*p'*) at 20kPa, until the satisfactory Skempton B value was reached

## IV. EQUIPMENT

*A. Triaxial apparatus*

A 50kN maximum capacity loading frame, equipped with water tight triaxial cells designed to withstand 2000kPa of water pressure, was used during experimentation. The system is instrumented with an external linear displacement Transducer (*LDS*), volume gauge (*VG*), pressure transducers (*PT*) for both cell and back pressure measurements and two internal linear variable differential transformers (*LVDT*) for small strain measurements. To accuretly measure the axial deformations to the samples and the travel distance for the shear waves, the LVDT's bodies were attached to a bottom pedestal and the transcoder's cores to a cup sitting on the sample (Fig.2).

*B. Bender elements*

Piezo-ceramic transducers in the form of the bender elements were incorporated within the triaxial cell to investigate the initial shear modulus evolution during the isotropic consolidation and a creep stage [6, 11 and 18]. BE transducers were fixed into the top and bottom plates of the triaxial cell. The method of BE results analysis is described and thoroughly discussed in Pennington' work [18]. The $G_0$ values obtained for the samples were calculated using the measured propagation velocity of the shear wave ($V_s$) and the bulk density ($\rho$) calculated for the samples (Eq.3).

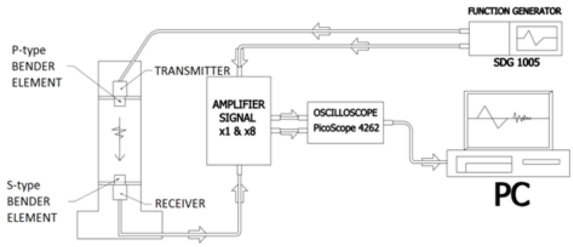


*Fig. 3. Bender elements signal acquisition.*

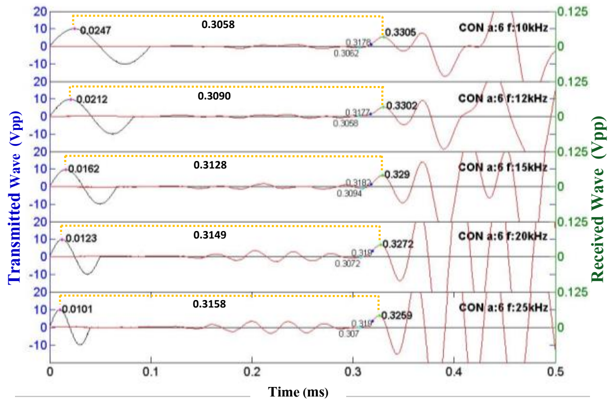


*Fig. 4. BE signal analysis.*

$$G_0 = \rho \cdot V_S^2 \tag{3}$$

The peak-to-peak (P-P) method of defining the arrival time of the shear wave was used for the experiments [11]. This method significantly reduces the variation in $G_0$ values measured for the successive consolidation stage affected by the near-field effect. Nonetheless, the P-P method can result in the underestimation of $V_s$, especially for waves with a longer period (*T*). Distortions to the arrival time, caused by the near-field effect, can be reduced by altering the frequency of the transmitted wave. Therefore, five sinusoidal waves of differing frequency (ranging from: 10–25 kHz) were used during the isotropic consolidation stage of every experiment (Fig.4). At the time of writing, it is not certain whether further corrections to the data will be required.

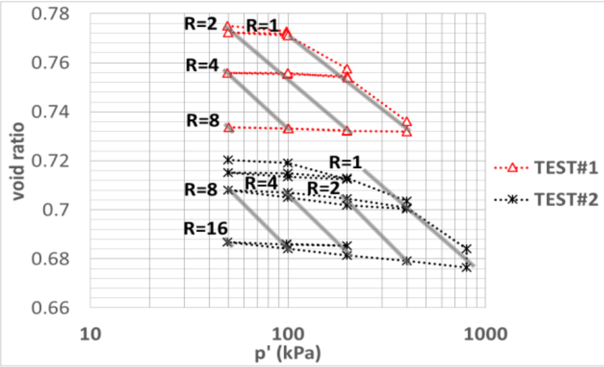


*Fig. 5.Isotropic compression test.*

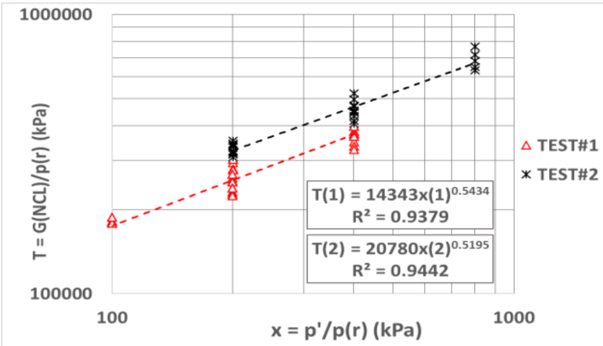


*Fig. 6 .Variation of the $G_0$ with stress.*

## V. TEST RESULTS

### A. Isotropic compression tests

To characterise the dependence between small strain stiffness and isotropic testing stress levels according to Eq.2 [14], the samples were subjected to successive isotropic loading and unloading cycles and bender measurements were taken at each points as presented in Fig.5. The two samples in Table.2 were subjected to isotropic pressures ranging between 50-800kPa, which resulted in the $R$ value ranging from 1 to 16. The line $R$=1 for both tests represents the isotropic normal compression line (*NCL*) with a slope (λ) and the values $N$ for the void ratio ($e$) at $p'$=1kPa presented in Table.2. The slope properties at $R$=1 were used to define the chalk's compressibility characteristics. In order to analyse the effect of $p'$ on the chalk's small strain stiffness at *NCL*, values of $p'$ lower than the preparation effective pressure ($p'_{prep}$) were removed (Table 2).

For normally consolidated samples with $R$=1, the values of $\log(G_{NCL}/p_r)$ against $\log(p'/p_r)$ are plotted in Fig.6, where a reference pressure ($p_r$) equals to 1kPa was assumed. For both samples, irrespective of the stress ratio, the power functions fit the data points well and show the gradual increase in the shear stiffness ($G_{NCL}$) at *NCL* with increasing $p'$. The vertical scatter in the data is the result of the five different frequencies adopted for the bender measurements. The measurements showed an overall trend of increasing in stiffness as the wave period ($T$) reduced. Following Eq.2 proposed by Viggiani and Atkinson [14], the trends in Fig.6 can be used to determine the value of the exponent $n^*$ for the investigated remoulded Margate chalk. Similar vlaues were detemrined for both samples with an average value $n^*$=0.531. This falls within the lower bound range indicated by the authors. The parameter $S^*$ in Eq.2 can be also derived from the data plotted in Fig.6 for the two samples. The obtained value for $S^*$ is higher than the values presented in authors' publication. However, as the plasticity index of the chalk (Table.1) is low, the hight magnitudes of the $S^*$ values were expected [14].

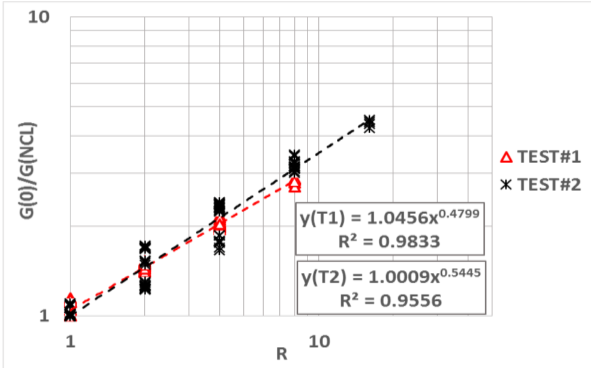


*Fig.7 . Variation of $G_0$ with stress and R ratio for reconstituted chalk samples.*

*Table 2. Results from isotropic compression tests.*

| Test No. | $p'_{prep}$ (kPa) | λ | N |
|---|---|---|---|
| TEST#1 | 64 | -0.027 | 0.919 |
| TEST#2 | 255 | -0.024 | 0.686 |

The unloading-reloading data for the tests shown in Fig.6 are presented in Fig.7. Again, the five frequencies shown in Fig.4 were used to obtain a more accurate relationship estimate. In this figure the data were plotted as $\log(G_0/G_{NCL})$ versus $\log(R)$. The normalisation of the $G_0$ by $G_{NCL}$ is done to eliminate the effect of $p'$ so that the effect of $R$ can be separately analysed. The slopes of the best fit lines ($m$) can be regarded as another soil parameter. The obtained data points for both experiments fall close to their best fit lines (aver. $R^2$=0.9695). The slope of the line through TEST#1 data is slightly shallower ($m$=0.4799) then the value obtained for that through TEST#2 ($m$=0.5445). This is due to the slight preliminary unloading of the applied confining stress. The values presented in both Fig.6 and Fig.7 define the stiffness parameters of crushed Margate chalk under isotropic stress condition. From analysing Eq.2, it can be concluded that the largest effect on the chalk's small strain stiffness is the soil parameter $S^*$, which magnitude is largely affected by the plasticity index of the soil [14]. Furthermore, both the parameters *m* and $n^*$ have similar magnitudes, but their effect on the stiffness differs. The influence of the exponent $(n)^*$ is much more pronounced. The *m* value presented in the paper has a higher magnitude than the values presented by other authors. This may be related to differnt particle shapes or other peculiarities of the material. The unloading-reloading slopes for both samples presented in Fig.5 are also very shallow. This very stiff response of the system could be explained by the wide range of particle sizes (Fig.1) and possible particle interlocking as described by [7].

*B. Maintained loading (creep) tests.*

The investigation of time dependent change of stiffness was performed by maintaining a constant isotropic stress levels and taking BE over set time intervals. Results form three diffent smapels are presented in this paper. All the samples were first subjected to $p'$=300kPa to overcome the vertical pressure imposed during sample preparation in the consolidometer.. Subsequently, to investigate the effect of *OCR*, two samples were unloaded to 200 and 100kPa respectively. For clearer comparison, the measured values for stiffness and sample vertical deformation will be expressed in terms of their percentage change from the initial value presented in Table.3.

*Table 3. Chalk samples at creep.*

| Test No. | *OCR* | Creep (days) | $n_{initial}$ | $d_{start}$ (mm) | $G(0)_{start}$ (MPa) |
|---|---|---|---|---|---|
| TEST#3 | 1.0 | 21 | 0.429 | 81.502 | 462 |
| TEST#4 | 1.5 | 23 | 0.423 | 81.456 | 339 |
| TEST#5 | 3.0 | 20 | 0.419 | 86.395 | 385 |

The deformation of the samples observed during the maintained stress stage are presented in Fig.8. In the figure, any positive percentage changes represents further consolidation of the samples. TEST#3 with *OCR*=1 has undergone solely consolidation whilst TEST#4 with *OCR*=1.5 has initially expanded and then started to creep. The initially observed larger deformation for TEST#3 can be attributed to the remnants of the primarily consolidation phase. The deformation results for TEST#5 were excluded from analysis as the LVDT sensors attached to the sample malfunctioned during testing. Nonetheless, based on the changes of sample deformation between TEST#3 and TEST#4, similar behaviour to TEST#4 is expected for TEST#5 with a more pronounced initial expansion and shallower creep. In Fig.9, the values of the percentage change of small strain shear modulus were plotted against the duration of the creep stage in days. All the samples, regardless of observed deformation in Fig.8, showed a stiffness improvement. The largest improvement of $G_0$ was achieved by the sample in TEST#3. The 18.4% increase to the initial stage value is ~2.4 times higher than the value from TEST#5. The main reason for this observation could be the reduction in $p'$, which would have resulted in arresting the processes responsible for sample deformation (Fig.8). Nevertheless, the gradual increase to the $G_0$ value in TEST#5 is still observed. The improvement in small strain stiffness during TEST#4 is comparable in behaviour to that during TEST#5. However, the observed deformation for both tests is significantly different (Fig.8). This suggests that the improvement to the stiffness may not be solely attributed to the sample creep deformation.

Fabricus [7], studying the burial diagenesis of chalk sediments, concluded that the primary consequence of the cementation process is a stiffness increase which may or may not be attributed to porosity loss. Therefore, using the information contained in the author's paper, it can be concluded that for the laboratory samples the recrystallization mechanism could be mobilised.

The values of porosity observed in the samples during the isotropic consolidations (Table 3) is very close to the maximum porosity ($n_{chalk}$=40%), where the dominant effect on the increase of sample stiffness is diminished. The large amount of the contact cement created during

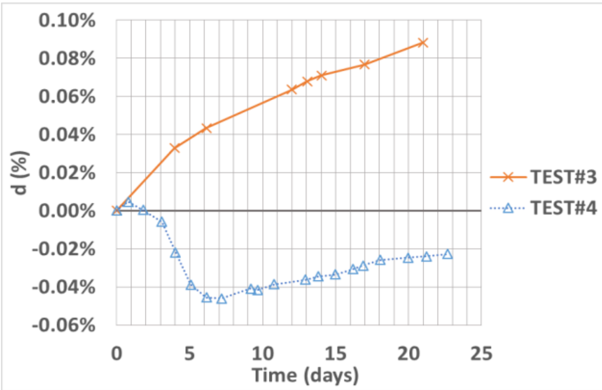


*Fig.8. Percentage change to the wave travel distance with time.*

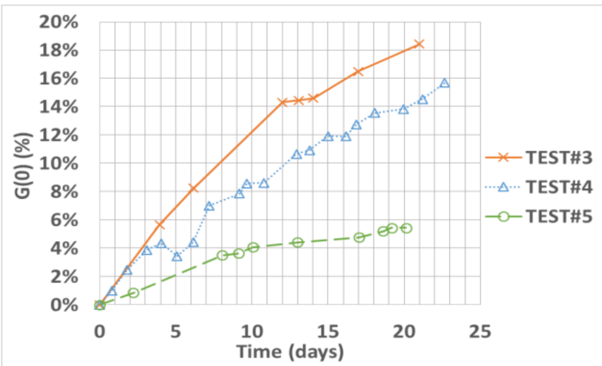


*Fig.9. Percentage change to the small strain stiffness with time.*

crushing could significantly accelerate the process of recrystallization. The very careful selection of the saturation liquid used for the sample preparation, as well as the material mineral composition itself, may have aided the curing process. Finally, as the degree of recrystallization is dependent on temperature, keeping the laboratory at a constant 22°C may have contributed to the observed increase in magnitude of $G_0$.

All of these above will cause the shear wave propagation velocity to rise and the reconstituted material will slowly start to regenerate the inter-particle bond.

## VI. CONCLUSION

The presented work investigated the time dependent evolution of the shear modulus of reconstituted Margate chalk under different stress states. Analysis of the consolidation results of the samples from bender elements tests has demonstrated the influence of the effective stress, the overconsolidation ratio and the dimensionless parameters on small strain stiffness. Good agreement is seen between the observed $n^*$ values with those found in the literature, confirming the importance of the plastic index on the soil stiffness. The magnitudes obtained for $S^*$ and $m$ were not within the bounds of previously published values, which was expected as particle geometry within the chalk and the interparticular locking both affect these values.

The effect of overconsolidation ratio on the creep has been identified. The increase in overconsoidation ratio value lowers, or in some cases even arrests the initial deformations of the chalk samples. Despite keeping effective stress constant, further consolidation within one of the overconsolidated samples was observed. This fact may indicate the involvement of other processes, such as the chemical bonding or perhaps the particle rearengment within the sample has been taking place.

Furthermore, under constant effective stress, a time dependent increase of the chalks' stiffness was observed for all samples, regardless of their overconsolidation ratio. As expected the largest increase to this value was seen for the normally consolidated sample.It also appears that, despite the case where the sample deformation was temporarily ceased, a steady increase to the soil stiffness was still observed. This may be linked partly to recrystallization within the chalk , which has been suggested by other authors. The increase in sample stiffness after 20 days was as high as 20%. Further tests and analysis are needed to completely ascertain the contrbutions of recrystallisation on sample strength and stiffness.

## REFERENCES


[1] C.R.I. Clayton, "The mechanical properties of the Chalk.". Chalk: proceedings of the International Chalk Symposium held at Brighton Polytechnic, 1990.

[2] J.A. Lord, C.R.I. Clayton, and R.N. Mortimore, "Engineering in chalk.", in C574. 2002, CIRIA.

[3] J.A. Lord, T. Hayward, and C.R.I. Clayton, "Shaft friction of CFA piles in chalk.", in Project report 86. 2003, CIRIA: London

[4] C.R.I. Clayton, "Some properties of remoulded Chalk.", In, 9th Institute Conference of Soil Mechanics and Foundation Engineering, 1977.

[5] J.M. Hancock, "The petrology of the Chalk.", Proceedings of the Geologists' Association, 1975. 86(4): p. 499-535.

[6] C.R.I. Clayton, "The Mechanical-Properties of the Chalk.", in proceedings of the International Chalk Symposium held at Brighton Polytechnic on 4-7 September, 1989. 1990, London, GB. p. 213-232.

[7] L.I. Fabricius, "How burial diagenesis of chalk sediments controls sonic velocity and porosity.", AAPG Bulletin, 2003. 87: p. 1755-1778.

[8] R.N. Mortimore, Logging the Chalk, 2014, Whittles Publishing: Dunbeath, Scotland, UK.

[9] R. Dyvik and C. Madshus, "Lab measurements of Gmax using bender elements.", Norges Geotekniske Institutt (NGI) publikasjon, 1986. 161: p. 6.

[10] D. Nash, M. Lings, and D. Pennington, "The dependence of anisotropic Go shear moduli on void ratio and stress state for reconstituted Gault clay.", in Pre-failure Deformation Characteristics of Geomaterials: Proc. 2nd Int. Symposium. 1999, Balkema: Turin. p. 229-238.

[11] TC-29, "International Parallel Test on the Measurement of Gmax Using Bender Elements Organized by TC-29.", S.F. Yamashita, T. Kawagushi, T. Mikami, T. Nakata, Y. Shibuya, S., Editor. 2005: Japanese Domestic Committee for TC-29. p. 76.

[12] C.R.I. Clayton, "Stiffness at small strain: research and practice.", Géotechnique, 2011. 61(1): p. 5-37.

[13] S. Rampello, G.M.B. Viggiani, and A. Amorosi, "Small-strain stiffness of reconstituted clay compressed along constant triaxial effective stress ratio paths.". Géotechnique, 1997. 47(3): p.475-489.

[14] G. Viggiani and J.H. Atkinson, " Stiffness of fine-grained soil at very small strains.". Géotechnique, 1995. 45(2): p. 249-265.

[15] R.C. Hartwig and R.H. Loeppert, "Pretreatment Effect on Dispersion of Carbonates in Calcareous Soils.", Soil Science Society of America, 1991. 55(1): p. 19-25.

[16] F. Storti and F. Balsamo, "Particle size distributions by laser diffraction: sensitivity of granular matter strength to analytical operating procedures.", Solid Earth, 2010. 1: p. 25-48.

[17] A.F. Hyde, T. Higuchi, and K. Yasuhara, "Liquefaction, cyclic mobility, and failure of silt", Journal of geotechnical and geoenvironmental engineering, 2006.

D.S. Pennington, "The anisotropic small strain stiffness of Cambridge Gault clay.", in Department of Civil Engineering. 1999, The University of Bristol.